

Probing Novel Physics through Pulsar Timing Arrays

Zu-Cheng Chen (陈祖成)

Collaborators: Qing-Guo Huang, Yu-Mei Wu, Chen Yuan, Xingjiang Zhu, N. D. Ramesh Bhat, Yi Feng, George Hobbs, Richard N. Manchester, Christopher J. Russell, R. M. Shannon, (PPTA Collaboration)

Based on: *PRD* 100 (2019) 8, 081301; *PRL* 124 (2020) 25, 251101; *Sci.China Phys.Mech.Astron.* 64 (2021) 12, 120412; *ApJ* 925 (2022) 1, 37; *Commun.Theor.Phys.* 74 (2022) 10, 105402; *ApJ* 936 (2022) 1, 20; *PRD* 106 (2022) 8, L081101 ; *PRD* 107 (2023) 4, 042003

Department of Astronomy, Beijing Normal University
Advanced Institute of Natural Sciences, Beijing Normal University at Zhuhai

Apr 04, 2023 © KIAA-PKU



北京師範大學
BEIJING NORMAL UNIVERSITY

Outline

- 1 Introduction

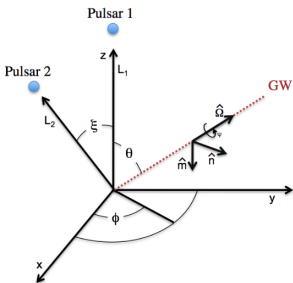
- 2 Probing Novel Physics with PTAs
 - Scalar-induced GW
 - Cosmic String
 - Ultralight Vector Dark Matter
 - Massive Gravity
 - Alternative Polarizations

- 3 Discussion

Time of Arrivals (TOAs)

$$\tau = \tau^{\text{TM}} + n = \tau^{\text{TM}} + \tau^{\text{RN}} + \tau^{\text{DM}} + \tau^{\text{WN}} + \tau^{\text{GW}}$$

- τ^{TM} – timing model: physical model for TOAs taking into account spin period, proper motion, binary orbital dynamics, etc.
- τ^{RN} – red noise (i.e. low-frequency correlated noise). Correlation timescales on the order of weeks - years.
- τ^{DM} : Model for time-varying dispersion measure variations (i.e. has $1/\nu^2$ dependence, where ν is the radio frequency).
- τ^{WN} – white noise: it is more than just a variance since we have data taken from different observing systems and different telescopes.
- τ^{GW} – GW signal.



- Redshift

$$z(t, \hat{\Omega}) = \frac{\nu_e - \nu_p}{\nu_p}$$

$$= \frac{\hat{p}^i \hat{p}^j}{2(1 + \hat{\Omega} \cdot \hat{p})} \left[h_{ij}(t_p, \hat{\Omega}) - h_{ij}(t_e, \hat{\Omega}) \right]$$

$$z(t) = \int_{S^2} d\hat{\Omega} z(t, \hat{\Omega})$$

- Timing residual in frequency-domain

$$\tilde{r}(f, \hat{\Omega}) = \frac{1}{2\pi i f} \left(1 - e^{-2\pi i f L(1 + \hat{\Omega} \cdot \hat{p})} \right) \times \sum_A h_A(f, \hat{\Omega}) F^A(\hat{\Omega})$$

- Antenna pattern

$$F^A(\hat{\Omega}) = e_{ij}^A(\hat{\Omega}) \frac{\hat{p}^i \hat{p}^j}{2(1 + \hat{\Omega} \cdot \hat{p})}$$

- Assume the GWB is isotropic, unpolarized, and stationary

$$\left\langle h_A^*(f, \hat{\Omega}) h_{A'}(f', \hat{\Omega}') \right\rangle = \frac{3H_0^2}{32\pi^3 f^3} \delta^2(\hat{\Omega}, \hat{\Omega}') \delta_{AA'} \delta(f - f') \Omega_{\text{gw}}(f)$$

- Spectrum of GWB

$$\Omega_{\text{gw}}(f) \equiv \frac{1}{\rho_{\text{crit}}} \frac{d\rho_{\text{gw}}}{d \ln f}, \quad \rho_{\text{crit}} = \frac{3H_0^2}{8\pi}, \quad \rho_{\text{gw}} = \frac{1}{32\pi} \left\langle \dot{h}_{ij}(t, \vec{x}) \dot{h}^{ij}(t, \vec{x}) \right\rangle,$$

- Cross-power spectral density

$$S_{IJ} = \left\langle \tilde{r}_I^*(f) \tilde{r}_J(f') \right\rangle = \frac{1}{\gamma} \frac{H_0^2}{16\pi^4 f^5} \delta(f - f') \Gamma_{IJ}(f, L_I, L_J, \xi) \Omega_{\text{gw}}(f)$$

- Overlap reduction function (ORF) is function of f, L_I, L_J, ξ

$$\Gamma_{IJ} = \gamma \sum_A \int d\hat{\Omega} \left(e^{2\pi i f L_I (1 + \hat{\Omega} \cdot \hat{p}_I)} - 1 \right) \times \left(e^{-2\pi i f L_J (1 + \hat{\Omega} \cdot \hat{p}_J)} - 1 \right) F_I^A(\hat{\Omega}) F_J^A(\hat{\Omega})$$

- Hellings & Downs correlations for $fL \gg 1$ (short-wavelength approximation)

$$\Gamma_{IJ} = \frac{3}{2} \left(\frac{1 - \cos \xi}{2} \right) \ln \frac{1 - \cos \xi}{2} - \frac{1 - \cos \xi}{8} + \frac{1}{2}$$

Common-spectrum process in PTAs

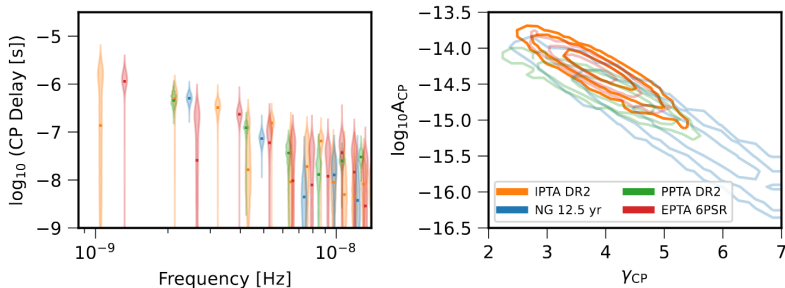


Figure 9. Comparison of IPTA DR2 to other recent data sets. *left:* Free spectral common-spectrum process model. The inclusion of legacy data not used in recent PTA analyses allows IPTA DR2 to reach lower frequencies despite missing the most recently collected data. *right:* 2D posterior for CP parameters log-amplitude and spectral index, where the contours represent the 1-, 2-, and 3- σ confidence intervals. All recent data sets are in broad agreement on the characteristics of a common-spectrum process.

- All four PTAs found a CP in their recent publicly released data set.
- Lacking evidence for HD correlations predicted by GR.

Arzoumanian, Zaven, et al., ApJL (2020); Goncharov, Boris, et al. ApJL (2021);

Chen, S., et al., MNRAS (2021); Antoniadis, J., et al., MNRAS (2022);

Scalar-Induced Gravitational Waves (SIGWs)

- Primordial perturbations can be generated by quantum fluctuations during inflation.
- Metric perturbation in Newtonian gauge

$$ds^2 = a^2 \left\{ -(1 + 2\phi)d\eta^2 + \left[(1 - 2\phi)\delta_{ij} + \frac{h_{ij}}{2} \right] dx^i dx^j \right\}, \quad (1)$$

where $\phi \equiv \phi^{(1)}$ and $h_{ij} \equiv h_{ij}^{(2)}$ are the scalar and tensor perturbations, respectively.

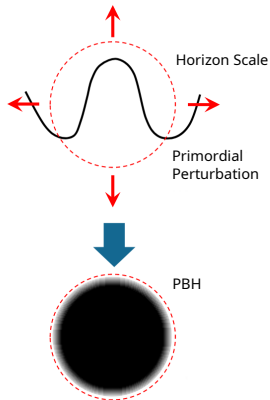
- Primordial scalar perturbation can be the source of SIGWs, as well as primordial black holes (PBHs).

Primordial black holes (PBHs)

- PBHs are formed in the early universe by gravitational collapse of primordial density perturbations
- PBH mass can span many orders

$$m_{\text{PBH}} \sim \frac{t}{G} \sim 10^{-18} \left(\frac{t}{10^{-23}} \right) M_{\odot} \quad (2)$$

- PBHs survived from Hawking radiation can be DM candidates.
- PBHs can explain LVK BBHs.



SIGW up to 3rd order

$$h''_{ij} + 2\mathcal{H}h'_{ij} - \nabla^2 h_{ij} = -4\mathcal{T}_{ij}^{\ell m} S_{\ell m}(\phi)$$

The source term $S_{\ell m}(\phi)$ needs to be expanded to 4th order!

$$\Omega_{\text{GW}}(\eta, k) = \frac{1}{\rho_c} \frac{d\rho_{\text{GW}}}{d \ln f} \propto \left\langle S^{(2)} S^{(2)} \right\rangle + \left\langle S^{(3)} S^{(3)} \right\rangle + \left\langle S^{(2)} S^{(4)} \right\rangle$$

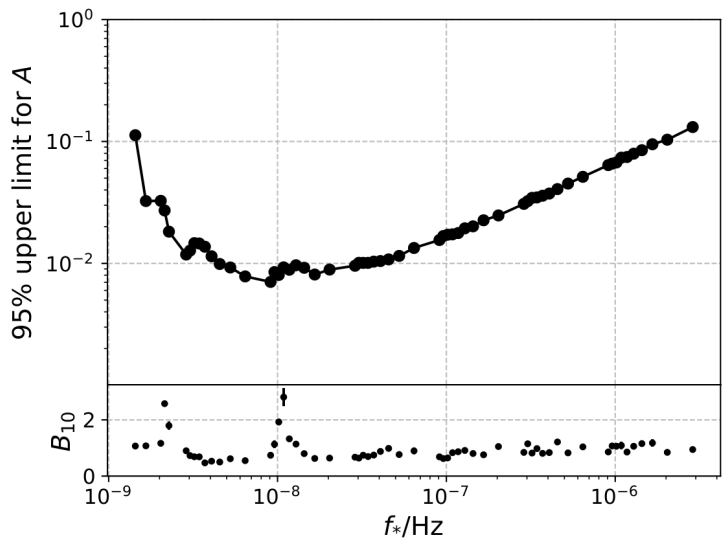
$$S_{ij}^{(2)} = 4\phi \partial_i \partial_j \phi + 2\partial_i \phi \partial_j \phi - \partial_i \left(\phi + \frac{\phi'}{\mathcal{H}} \right) \partial_j \left(\phi + \frac{\phi'}{\mathcal{H}} \right)$$

$$S_{ij}^{(3)} = \frac{1}{\mathcal{H}} \left(12\mathcal{H}\phi - \phi' \right) \partial_i \phi \partial_j \phi - \frac{1}{\mathcal{H}^3} \left(4\mathcal{H}\phi - \phi' \right) \partial_i \phi' \partial_j \phi' \\ + \frac{1}{3\mathcal{H}^4} \left(2\partial^2 \phi - 9\mathcal{H}\phi' \right) \partial_i \left(\mathcal{H}\phi + \phi' \right) \partial_j \left(\mathcal{H}\phi + \phi' \right)$$

$$S_{ij}^{(4)} = 16\phi^3 \partial_i \partial_j \phi + \frac{1}{3\mathcal{H}^3} \left[2\phi' \partial^2 \phi - 9\mathcal{H}\phi'^2 - 8\mathcal{H}\phi \partial^2 \phi + 18\mathcal{H}^2 \phi \phi' + 96\mathcal{H}^3 \phi^2 \right] \partial_i \phi \partial_j \phi \\ + \frac{2}{3\mathcal{H}^5} \left[-\phi' \partial^2 \phi + 3\mathcal{H}\phi'^2 + 4\mathcal{H}\phi \partial^2 \phi + 3\mathcal{H}^2 \phi \phi' - 12\mathcal{H}^3 \phi^2 \right] \partial_i \phi' \partial_j \phi' \\ + \frac{1}{36\mathcal{H}^6} \left[-16(\partial^2 \phi)^2 - 3\partial_k \phi' \partial^k \phi' + 120\mathcal{H}\phi' \partial^2 \phi - 6\mathcal{H}\partial_k \phi \partial^k \phi' \right. \\ \left. + 144\mathcal{H}^2 \phi \partial^2 \phi - 180\mathcal{H}^2 \phi'^2 + 33\mathcal{H}^2 \partial_k \phi \partial^k \phi - 504\mathcal{H}^3 \phi \phi' - 144\mathcal{H}^4 \phi^2 \right] \\ \times \partial_i \left(\mathcal{H}\phi + \phi' \right) \partial_j \left(\mathcal{H}\phi + \phi' \right)$$

Chen Yuan, ZCC, Qing-Guo Huang, PRD Rapid Communications (2019)

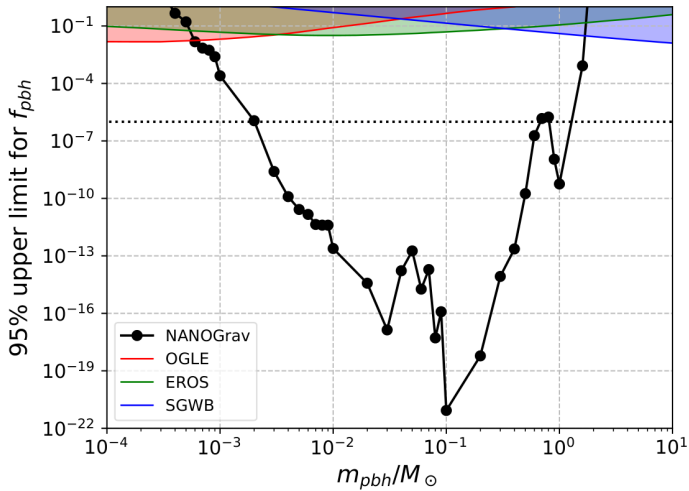
Constrain primordial scalar perturbation with NANOGrav 11-yr data set



ZCC, Chen Yuan, Qing-Guo Huang, PRL (2020)

Constrain PBH with NANOGrav 11-yr data set

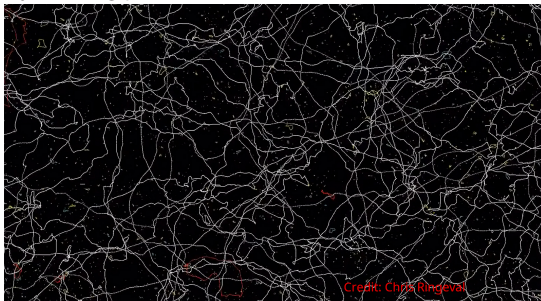
$$f_{\text{pbh}} \equiv \frac{\Omega_{\text{pbh}}}{\Omega_{\text{CDM}}} \simeq 1.9 \times 10^7 (1/A - 1) e^{-\frac{1}{2A}} \left(\frac{m_{\text{pbh}}}{M_{\odot}} \right)^{-1/2}$$



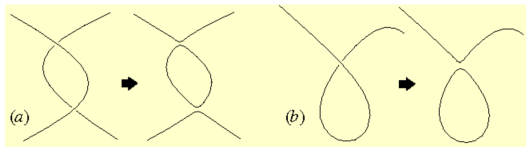
ZCC, Chen Yuan, Qing-Guo Huang, PRL (2020)

Cosmic String

- Cosmic strings are linear topological defects that can form in the early Universe from symmetry-breaking phase transitions.



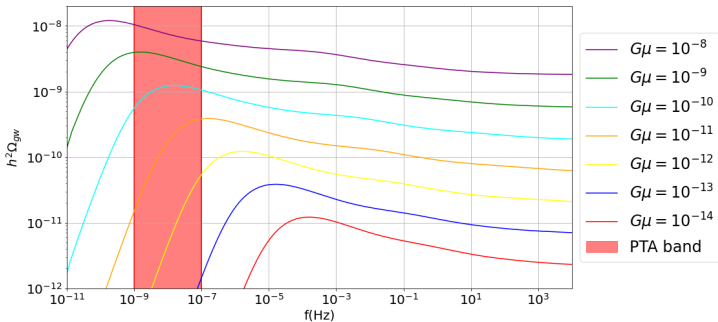
- The intersection between cosmic strings can lead to reconnections and form loops, which will then decay due to relativistic oscillation and emit gravitational waves.



Cosmic string loop formation. A loop forms (a) when two strings interact in 2 separate points or (b) when a string crosses itself.

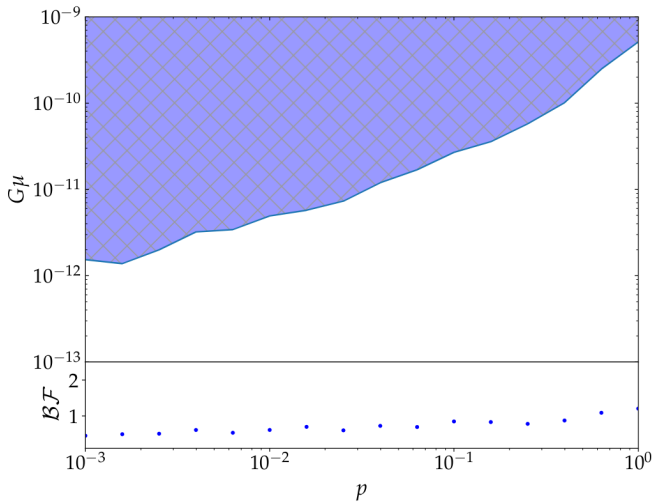
© Cambridge cosmology group

GW energy density spectrum of cosmic strings



- Here, $p = 1$ is the reconnection probability.
- $G\mu$ is string tension – the energy stored per unit length.

Constraining cosmic string with PPTA DR2



ZCC, Yu-Mei Wu, Qing-Guo Huang, *ApJ* (2022)

Ultralight Vector Dark Matter (UVDM)

- Ultralight vector field with mass $\sim 10^{-22}$ eV can be DM candidate.
- The vector field oscillating coherently on galactic scales induces oscillations of the spacetime metric with a frequency around nHz, which is detectable by PTAs.
- Action for a free massive vector field

$$S = \int d^4x \sqrt{-g} \left(-\frac{1}{4} F^{\mu\nu} F_{\mu\nu} - \frac{1}{2} m^2 A_\mu A^\mu \right), \quad (3)$$

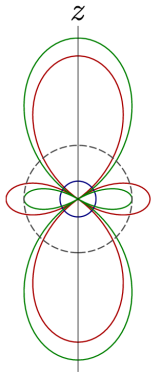
where $F_{\mu\nu} = \partial_\mu A_\nu - \partial_\nu A_\mu$.

- Only longitudinal mode survives during inflation

$$A_{\hat{k}}(t, \mathbf{x}) = A(\mathbf{x}) \cos(mt + \alpha(\mathbf{x})). \quad (4)$$

where $\hat{k} = (\sin \theta \cos \phi, \sin \theta \sin \phi, \cos \theta)$ is the oscillating direction.

Redshift induced by UVDM



$$ds^2 = \eta_{\mu\nu} dx^\mu dx^\nu - 2\Phi(t, \mathbf{x}) dt^2 + 2\Psi(t, \mathbf{x}) \delta_{ij} dx^i dx^j + h_{ij}(t, \mathbf{x}) dx^i dx^j$$

$$\Psi(t, \mathbf{x}) = \Psi_0(\mathbf{x}) + \Psi_{\text{osc}}(\mathbf{x}) \cos(2mt + 2\alpha(\mathbf{x}))$$

$$z_\Psi(t) = \Psi_{\text{osc}}(\mathbf{x}_e) \cos(2mt + 2\alpha(\mathbf{x}_e)) - \Psi_{\text{osc}}(\mathbf{x}_p) \cos[2m(t - |\mathbf{x}_p|) + 2\alpha(\mathbf{x}_p)]$$

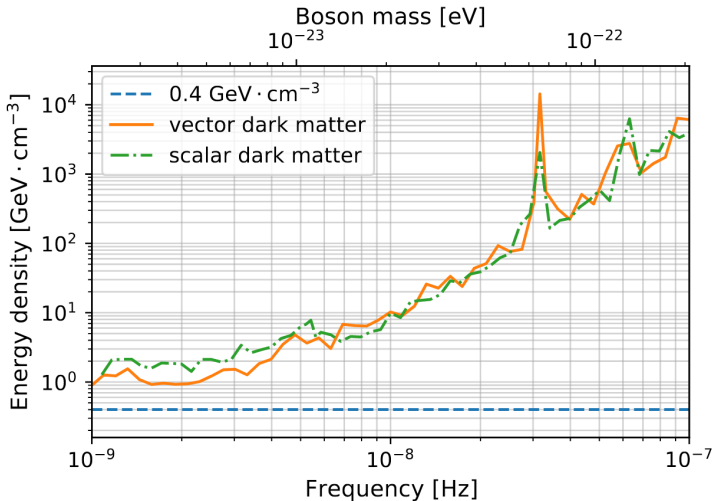
$$h_{ij}(t, \mathbf{x}) = h_{\text{osc}}(\mathbf{x}) \cos(2mt + 2\alpha(\mathbf{x})) (\hat{l} \otimes \hat{l} + \hat{n} \otimes \hat{n} - 2\hat{k} \otimes \hat{k}),$$

$$z_h(t) = \frac{1}{2} \hat{p}^i \hat{p}^j [h_{ij}(t, \mathbf{x}_e) - h_{ij}(t - |\mathbf{x}_p|, \mathbf{x}_p)],$$

The redshift is angular dependent because of the oscillation of UVDM. The blue line and red line represent the contribution of the trace part $z_\Psi(t)$ and the traceless part $z_h(t)$, respectively. Actually, we only observe the summation of z_Ψ and z_h , which is depicted by the green line. The angle θ is measured from the direction of the oscillation chosen as the z-axis. A gray dashed line shows the magnitude of the redshift when the DM is a scalar field.

Kimihito Nomura, Asuka Ito, Jiro Soda, EPJC (2020)

Constraining UVDM with PPTA DR2



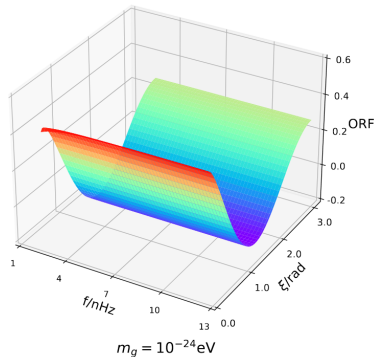
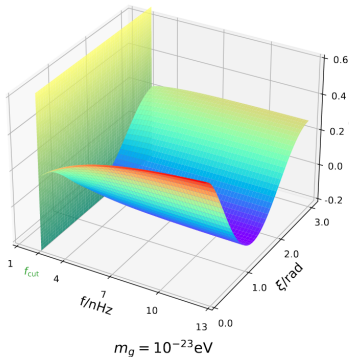
Yu-Mei Wu, ZCC, Qing-Guo Huang, Xingjiang Zhu, et. al., PRD Letter (2022)

Massive Gravity

- Massive gravity is a theory of gravity endowing the graviton with a nonzero mass.
- Fierz-Pauli mass term (1939)

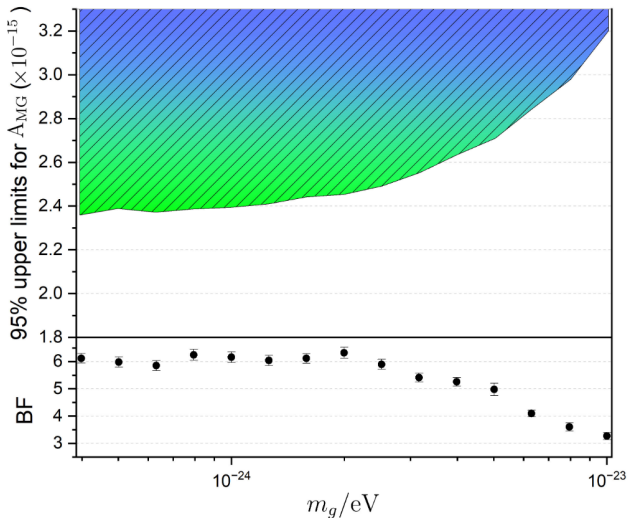
$$S_{\text{FP}} = \int \frac{1}{2} m_g^2 (h_{\mu\nu} h^{\mu\nu} - h^2) d^4x \quad (5)$$

- Overlap reduction function for the tensor mode [$f_{\text{cut}} \equiv m_g c^2 / (2\pi\hbar)$]



Qiyue Liang, Mark Trodden, *PRD* (2021); Yu-Mei Wu, ZCC, Qing-Guo Huang, *PRD* (2023)

Search for GWB from massive gravity in NANOGrav 12.5-yr data set

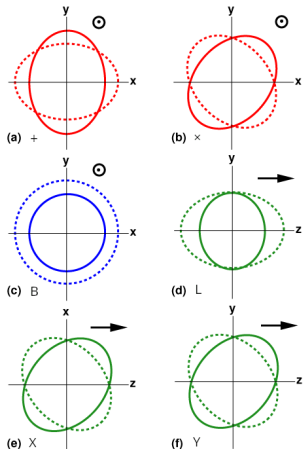


- Lighter graviton mass is preferred.

Yu-Mei Wu, ZCC, Qing-Guo Huang, PRD (2023)

Alternative Polarizations

Gravitational-Wave Polarization



- A general metric gravity theory in 4D spacetime can have 6 polarization modes.
- polarization tensors

$$\epsilon_{ij}^+ = \hat{m} \otimes \hat{m} - \hat{n} \otimes \hat{n},$$

$$\epsilon_{ij}^{\times} = \hat{m} \otimes \hat{n} + \hat{n} \otimes \hat{m},$$

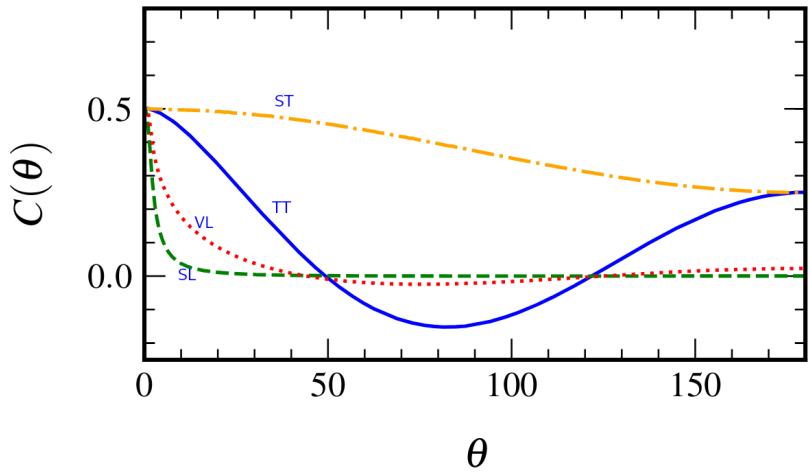
$$\epsilon_{ij}^B = \hat{m} \otimes \hat{m} + \hat{n} \otimes \hat{n},$$

$$\epsilon_{ij}^L = \hat{\Omega} \otimes \hat{\Omega},$$

$$\epsilon_{ij}^X = \hat{m} \otimes \hat{\Omega} + \hat{\Omega} \otimes \hat{m},$$

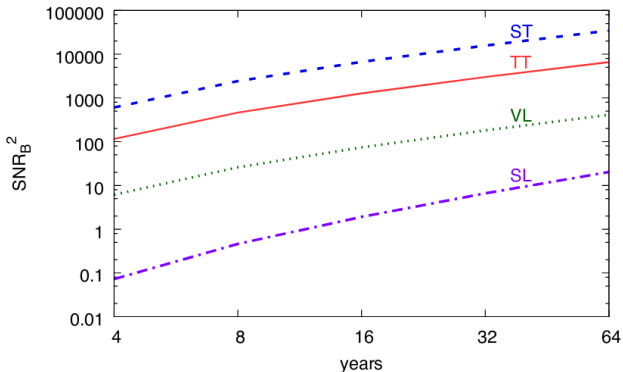
$$\epsilon_{ij}^Y = \hat{n} \otimes \hat{\Omega} + \hat{\Omega} \otimes \hat{n}$$

ORF



$$|\Gamma_{ST}| > |\Gamma_{TT}| > |\Gamma_{VL}| > |\Gamma_{SL}|$$

$$\text{SNR}_B^2 = 2 \sum_f \sum_a^{N_p} \sum_{b>a}^{N_p} \frac{\Gamma_{ab}^{I^2}(f)}{\Gamma_{aa}^I(f)\Gamma_{bb}^I(f) + \Gamma_{ab}^I(f)}.$$



ST is the easiest to detect among the four polarization modes.

Neil J. Cornish, Logan O'Beirne, Stephen R. Taylor, Nicolás Yunes, PRL 120 (2018)

Evidence for the ST correlations in NANOGrav 12.5-yr

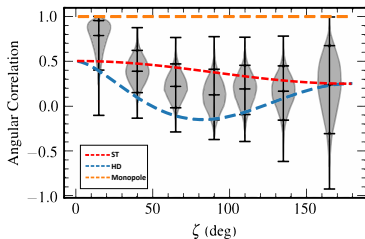
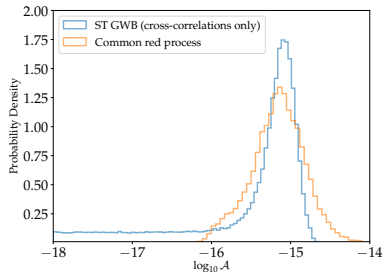
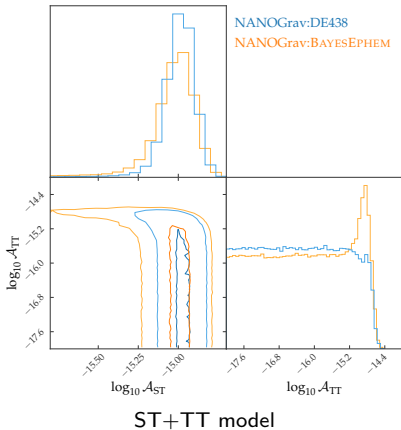
\mathcal{BF} compared to the UCP model with $\gamma_{\text{UCP}} = 13/3$.

ephemeris	TT	ST	VL	SL	ST+TT
DE438	4.96(9)	107(7)	1.94(3)	0.373(5)	96(3)
BAYESEPHM	2.35(3)	18.4(7)	1.31(2)	0.555(7)	16.7(3)

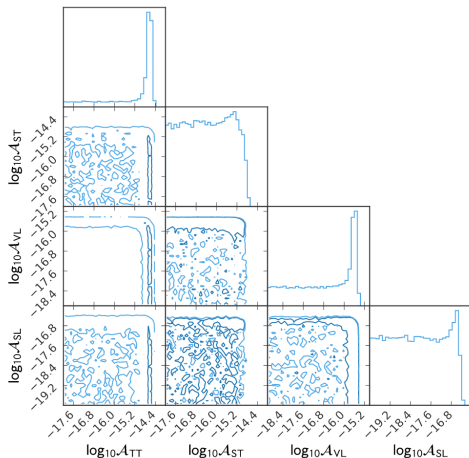
- No significant evidence for TT/VL/SL modes
- Strong Bayesian evidence for ST correlations;
- No TT correlations in addition to the ST mode;
- The evidence decreases when considering the BAYESEPHM model.

ZCC, Chen Yuan, Qing-Guo Huang, *Sci.China Phys.Mech.Astron.* (2021)

Evidence for the ST correlations in NANOGrav 12.5-yr

ZCC, Chen Yuan, Qing-Guo Huang, *Sci.China Phys.Mech.Astron.* (2021)

Constrain GW Polarization with PPTA DR2



Model	TT	ST	VL	SL
BF	2.15(4)	0.183(3)	1.06(2)	0.362(6)

No significant evidence for TT/ST/VL/SL correlations.

$$\mathcal{A}_{\text{TT}} \lesssim 3.0 \times 10^{-15}$$

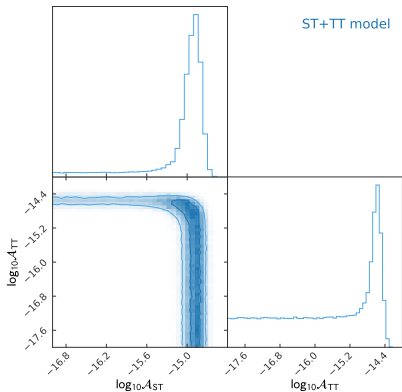
$$\mathcal{A}_{\text{ST}} \lesssim 1.0 \times 10^{-15}$$

$$\mathcal{A}_{\text{VL}} \lesssim 3.0 \times 10^{-16}$$

$$\mathcal{A}_{\text{SL}} \lesssim 2.7 \times 10^{-17}$$

Yu-Mei Wu, ZCC, Qing-Guo Huang, *ApJ* (2022)

Evidence for the ST correlations in IPTA DR2



Model	TT	ST	ST+TT
$\ln \mathcal{BF}$	2.53(3)	3.39(4)	3.63(4)

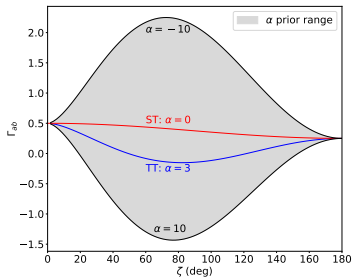
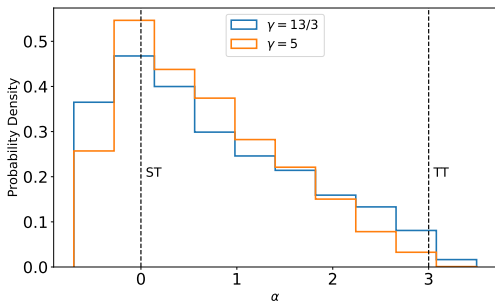
- Strong evidence for ST correlations.
- No significant evidence for an additional TT correlations.

ZCC, Yu-Mei Wu, Qing-Guo Huang, CTP (2022)

We also consider a parameterized transverse ORF as

$$\Gamma_{ab}(f) = \frac{1}{8} (3 + 4\delta_{ab} + \cos \xi_{ab}) + \frac{\alpha}{2} k_{ab} \ln k_{ab}. \quad (6)$$

ST: $\alpha = 0$ TT: $\alpha = 3$ prior of α : Uniform(-10, 10)



- ST mode is favored by IPTA DR2.
- TT mode is ruled out at 90% credible interval.

ZCC, Yu-Mei Wu, Qing-Guo Huang, CTP (2022)

Summary for the results of alternative polarizations

PTA	UCP	TT	ST	VL	SL	Monopole	Dipole
NANOGrav 12.5-yr	✓	✗	✓	✗	✗	✗	✗
PPTA DR2	✓	✗	✗	✗	✗	✗	✗
IPTA DR2	✓	✗	✓	N/A	N/A	✗	✗

- All three PTAs support the evidence for a common process, but the evidence for TT correlations is insignificant.
- NANOGrav 12.5-yr and IPTA DR2 indicate the common process has ST correlations, and the obtained \mathcal{A}_{ST} is consistent with the upper limit from PPTA DR2.

	NANOGrav 12.5-yr	PPTA DR2	IPTA DR2
\mathcal{A}_{ST}	$1.06^{+0.35}_{-0.28} \times 10^{-15}$	$\lesssim 1.8 \times 10^{-15}$	$1.29^{+0.51}_{-0.44} \times 10^{-15}$

Response from NANOGrav Collaboration

THE ASTROPHYSICAL JOURNAL LETTERS, 923:L22 (18pp), 2021 December 20

<https://doi.org/10.3847/2041-8213/ac401c>

© 2021. The Author(s). Published by the American Astronomical Society.

OPEN ACCESS



The NANOGrav 12.5-year Data Set: Search for Non-Einsteinian Polarization Modes in the Gravitational-wave Background

The NANOGrav Collaboration

Abstract

We search NANOGrav's 12.5 yr data set for evidence of a gravitational-wave background (GWB) with all the spatial correlations allowed by general metric theories of gravity. We find no substantial evidence in favor of the existence of such correlations in our data. We find that scalar-transverse (ST) correlations yield signal-to-noise ratios and Bayes factors that are higher than quadrupolar (tensor-transverse, TT) correlations. Specifically, we find ST correlations with a signal-to-noise ratio of 2.8 that are preferred over TT correlations (Hellings and Downs correlations) with Bayesian odds of about 20:1. However, the significance of ST correlations is reduced dramatically when we include modeling of the solar system ephemeris systematics and/or remove pulsar J0030+0451 entirely from consideration. Even taking the nominal signal-to-noise ratios at face value, analyses of simulated data sets show that such values are not extremely unlikely to be observed in cases where only the usual

produce.

LIGO and VIRGO have already made possible a number of GW tests of general relativity (Abbott et al. 2016a, 2016b, 2017a, 2017b, 2018a, 2018b, 2019a, 2019b, 2020a, 2020b, 2020c, 2021a, 2021b). Until very recently (Chen et al. 2021a, 2021b; Wu et al. 2021b), PTA data had not been used to perform GW tests of gravity

due to the absence of a strong signal that can be attributed to GWs. However, as we mentioned, this situation has changed (see NG12.5 and Goncharov et al. 2021). Even though NANOGrav's 12.5 yr data set did not contain strong evidence for quadrupolar correlations, the detection of a common red noise process brings PTAs to a regime where the exploration of non-Einsteinian theories could prove to be fruitful.

of a detection of any polarization mode of gravity, we place an index of $\gamma = 5$ and a reference frequency of $f_{\text{yr}} = 1 \text{ yr}^{-1}$. Among a set of metric theories of gravity, we find the values of $4 \pm 0.03 \times 1$

As shown in Figure 9, the most favored Bayesian model is a GWB with GW-like monopolar correlations of Equation (25) with a Bayes factor greater than 100. Additionally, as a cross-check, we have reproduced the results of Chen et al. (2021a), where a model with ST correlations with a spectral index of 5, [ST]M3A[5], was compared to a model without correlations and a spectral index of 13/3, M2A[13/3]. We obtain a Bayes factor of about 94 in favor of [ST]M3A[5], which is consistent with their results.

Summary and Discussion

- PTAs are a unique and powerful tool to detect the nHz GWs.
- There is little evidence for Hellings-Downs curve that defines the angular correlation of a tensorial transverse signal.
- The null-detection has constrained a variety of physical models, including
 - Scalar-induced GW and PBH
 - Cosmic string
 - Ultralight vector DM
 - Massive gravity
- A scalar transverse signal seems to be preferred by NANOGrav 12.5-yr data set and IPTA DR2, if a stochastic signal is at all present.